A stochastic approach for generating spectrum compatible fully nonstationary earthquakes

by

Pierfrancesco Cacciola

School of Environment and Technology, University of Brighton, Cockcroft building, Lewes road, Brighton BN24GJ, UK

ABSTRACT: Simulation of artificial earthquakes in agreement with the provision of international seismic codes is addressed. Due to the importance of nonstationary frequency content on the seismic assessment of structures, in this paper a new method for generating spectrum compatible fully nonstationary earthquakes is proposed. The method assumes that the ground motion is modeled by the superposition of two contributions: the first one is a fully nonstationary counterpart modeled by a recorded earthquake; the second one is a corrective random process adjusting the recorded earthquake in order to make it spectrum compatible. Several examples show the accuracy of the proposed method.

Keywords: spectrum compatible, earthquakes, nonstationary, stochastic process, evolutionary power spectral density.

1 INTRODUCTION

For a number of applications connected with the seismic assessment of structures it is necessary to generate accelerograms which are compatible with a design response spectrum. To date, international seismic codes [1,2] do not give a method for generating the time-histories imposing only the matching of the mean simulated response spectrum with the target one according to certain spectrum compatible criteria. As a consequence, several methods have been proposed in literature coping with the generation of spectrum compatible accelerograms. Earlier contributions on this subject can be found in [3]. Based on either a deterministic or stochastic approaches two main parallel strategies are usually adopted for defining suitable earthquake time histories. Namely, based on a deterministic approach the spectrum compatible accelerogram is usually determined via an iterative alteration of the frequency content of synthetic or recorded time-histories. In reference [4] a single spectrum compatible accelerogram using an artificial deterministic signal resulting by the superposition of a number of harmonics with amplitude scaled so as to mach the target response spectrum has been determined. Neural network based approach for generating accelerograms through the knowledge of the inverse mapping from response spectra to earthquake accelerograms is proposed in [5]. Wavelet-based methods modifying recorded accelerograms such that those are compatible with a given response spectrum can be found in [6-8].

Deterministic-based approach possesses the advantage to lead generally to spectrum compatible accelerograms nonstationary in both amplitude and frequency; on the other hand it suffers the major drawback to produce a single spectrum compatible accelerogram from and individual recorded signal. Therefore since for design purpose it is re-

quired [1,2] the use of a number of accelerograms the application of a deterministic approach could be prohibitive whereas few records are allowable.

Furthermore, being the response spectrum determined smoothing and averaging the response spectra pertinent to a number of recorded signals and due to the widely recognized random nature of the seismic action, stochastic approach appears more attractive. In this regard, many common approaches rely on modeling the seismic action as a realization of a stationary or quasi-stationary stochastic process. Moreover, in the framework of stochastic dynamics, spectral representation of random processes is usually preferred. Accordingly, by modeling the seismic input as a stationary Gaussian process, the spectrum compatible power spectral density is first determined. Vanmarcke and Gasparini [9] pointed-out the fundamental relationship between the response spectrum and the power spectral density of the input via the so-called "first passage problem". Based on this relationship various procedures have been proposed in literature for determining the spectrum compatible power spectral density. (see e.g. ref. [9-18]). An iterative scheme to generate seismic ground motion time histories at several location on the ground surface that are compatible with prescribed response spectra correlated according to a given coherence function has been proposed in [19]. After determining the power spectral density of the base acceleration, samples of spectrum compatible time histories can be simulated through the superposition of harmonics with random phase [20]. Even if the above described approaches represent the seismic action reliably reflecting its inherent random nature, it suffers the major drawback of neglecting the nonstationary characteristics of the real records. Remarkably, it is well known that the dynamic response of nonlinear structures is highly influenced by the nonstationary behavior of the input [21,22]. Thus, more reliable simulations have to take into account the time variability of

both intensity and frequency content of the ground motion. Considering an earthquake time history as a realization of a nonstationary stochastic process Spanos and Vargas Loli [23] derived an approximate analytical expression of the spectrum compatible evolutionary power spectrum. The simulated time-histories are iteratively adjusted a posteriori in order to match the response spectrum. Generation of nonseparable artificial earthquake accelerograms has been also proposed in [24]. The method assume an empirical model of the evolutionary power spectral density function possessing the feature that high frequency component are magnified in the early part of the process and the iterative correction of the simulated accelerograms. Nonstationary characteristics from recorded earthquakes have been taken into account in [25] by means of phase spectrum for generating spectrum compatible signals. Ensemble of spectrum compatible accelerograms using stochastic neural networks has been proposed in [26]. Recently, the procedure originally established in Spanos and Vargas Loli [23] has been modified by Giaralis and Spanos [27] by means of the use of harmonic wavelets transform for iteratively improve the matching between the target and the simulated response spectra.

In this paper a method based on the spectral representation of stochastic processes is proposed. The method assumes that the ground motion is modeled by the superposition of two contributions: the first one is a fully-nonstationary counterpart modeled by a recorded earthquake, that takes into account the time variability of both intensity and frequency content; the second one is a corrective term represented by a quasi-stationary process adjusting the response spectrum of the nonstationary signal in order to make it spectrum compatible. Remarkably, the simulated earthquakes do not require any further iterative correction leading the proposed procedure very handy and competitive from a computational point of view. Therefore, the influence of the corrective term on the non-

stationary behavior of the original recorded signal has been scrutinized via a pertinent study of the mean instantaneous energy and frequency of the spectrum compatible earthquakes. Various examples show the accuracy and the efficiency of the proposed method.

2 GENERATING QUASI-STATIONARY SPECTRUM COMPATIBLE EARTHQUAKES

Assume that a target pseudo-acceleration response spectrum $RSA(\omega_0, \zeta)$ (for a given natural frequency, ω_0, and damping ratio, ζ) is specified. The problem of simulating spectrum compatible earthquakes is addressed on a probabilistic basis under the assumption that an earthquake time history is considered as a realization of a random process. In this section the simplest hypothesis of zero-mean stationary Gaussian random process, fully defined by the so-called power spectral density function, is assumed. Accordingly, the problem is recast to determine the power spectral density function whose response spectrum match the target one. This can be pursued via the following first crossing problem [9]

$$RSA(\omega_0, \zeta) = \omega_0^2 \eta_U (T_s, p = 0.5; \lambda_{0,U}(\omega_0, \zeta), \lambda_{1,U}(\omega_0, \zeta), \lambda_{2,U}(\omega_0, \zeta)) \sqrt{\lambda_{0,U}(\omega_0, \zeta)}, \qquad (1)$$

where η_U is the peak factor given by the equation

$$\eta_U = \sqrt{2\ln\left\{2N_U\left[1 - exp\left[-\delta_U^{1,2}\sqrt{\pi \ln\left(2N_U\right)}\right]\right]\right\}}, \qquad (2)$$

with

$$N_U = \frac{T_s}{2\pi}\sqrt{\frac{\lambda_{2,U}(\omega_0,\zeta)}{\lambda_{0,U}(\omega_0,\zeta)}}\left(-\ln p\right)^{-1} \ , \tag{3}$$

and

$$\delta_U = \sqrt{1-\frac{\lambda_{1,U}(\omega_0,\zeta)^2}{\lambda_{0,U}(\omega_0,\zeta)\lambda_{2,U}(\omega_0,\zeta)}} \ , \tag{4}$$

where T_s is the time observing window, and p is the not-exceeding probability. Furthermore , $\lambda_{i,U}(\omega_0,\zeta)$ $(i=0,1,2)$ are the response spectral moments defined as

$$\lambda_{i,U}(\omega_0,\zeta) = \int_0^\infty \omega^i \left|H(\omega,\omega_0,\zeta)\right|^2 G_{\ddot{u}_g}(\omega)d\omega \ , \tag{5}$$

in which $\left|H(\omega,\omega_0,\zeta)\right|^2 = \left((\omega_0^2-\omega^2)^2+4\zeta^2\omega_0^2\omega^2\right)^{-1}$ is the energy transfer function and $G_{\ddot{u}_g}(\omega)$ is the unilateral power spectral density function of the ground acceleration process that have to be determined. It is noted also that in eq. (1) the 50% fractile has been approximated by the mean value of the peak values.

A handy recursive expression determining the power spectral density compatible with a given response spectrum has been proposed in reference [18]. Specifically,

$$G_{\ddot{u}_g}\left(\omega\right) = 0 \qquad 0 \le \omega \le \omega_l \ , \tag{6}$$

$$G_{\ddot{u}_g}(\omega_i) = \frac{4\zeta}{\omega_i\pi - 4\zeta\omega_{i-1}}\left(\frac{RSA(\omega_i,\zeta)^2}{\eta_U^2(\omega_i,\zeta)} - \Delta\omega\sum_{j=1}^{i-1} G_{\ddot{u}_g}(\omega_j)\right), \quad \omega > \omega_l \tag{7}$$

where the peak factor η_U is given by equation (2) along with the following approximate parameters

$$N_U = \frac{T_s}{2\pi}\omega_i \left(-\ln p\right)^{-1} , \tag{8}$$

$$\delta_U = \left[1 - \frac{1}{1-\zeta^2}\left(1 - \frac{2}{\pi}\arctan\frac{\zeta}{\sqrt{1-\zeta^2}}\right)^2\right]^{1/2} , \tag{9}$$

determined assuming that the input PSD possess a smooth shape and $\zeta << 1$. Moreover $\omega_l \cong 1$ rad/seç is the lowest bound of the existence domain of η_U. The accuracy of eqs. (6) and (7) can be also improved via the following iterative scheme [9]

$$G_{\ddot{u}_g}{}^{(j)}(\omega) = G_{\ddot{u}_g}{}^{(j-1)}(\omega)\left[\frac{RSA(\omega,\zeta)^2}{\widetilde{RSA}^{(j-1)}(\omega,\zeta)^2}\right], \tag{10}$$

$\widetilde{RSA}^{(j)}$ being the approximate pseudo-acceleration spectrum determined at the *j*-th iteration through equations (1-5).

After determining the spectrum compatible power spectral density $G_{\ddot{u}_g}(\omega)$ the simulation of spectrum compatible ground acceleration earthquakes is performed via the superposition of N_a harmonics with random phases. Specifically, the *k*-th artificial earthquake is given by the equation

$$\ddot{u}_g^{(k)}(t) = \varphi(t)\sum_{i=1}^{N_a}\sqrt{2G_{\ddot{u}_g}(i\,\Delta\omega)\Delta\omega}\cos(i\,\Delta\omega t + \phi_i^{(k)}) , \tag{11}$$

where $\phi_i^{(k)}$ are independently random phases uniformly distributed in the interval $[0, 2\pi)$ and $\varphi(t)$ is a modulating function. In order to preserve the stationary condition of the response process within a segment of duration T_s (i.e. the time-observing window), the modulating function proposed in [28] is selected. That is,

$$\varphi(t) = \begin{cases} \left(\dfrac{t}{t_1}\right)^2 & t < t_1 \\ 1 & t_1 \le t \le t_2 \\ \exp\left[-\beta\left(t - t_2\right)\right] & t > t_2 \end{cases} \tag{12}$$

with $t_2 = t_1 + T_s$.

Remarkably, Using this approach the spectrum compatible criteria provided by seismic codes are satisfied [18]. So that the earthquake ground acceleration samples generated using equations (6-12) can be used for design applications.

3 GENERATING FULLY NON-STATIONARY SPECTRUM COMPATIBLE EARTHQUAKES: PROPOSED METHOD

To date, the suite of artificial accelerograms established by seismic codes is based on the positive matching of the simulated response spectrum with the target one. No rules have been imposed regarding the duration, the input energy, the stationary or nonstationary behaviour of the simulated time-histories. On the other hand, the importance of non-stationary frequency content on the response of nonlinear structures has been manifested in various studies [21,22]. Thus, more reliable simulations have to take into account the time variability of the frequency content of the ground motion.

According to that, in this paper a new strategy for simulating spectrum compatible fully nonstationary earthquakes is proposed. To this aim, it is assumed that the nonstationary spectrum compatible earthquake is modeled by the superposition of two contributions: the first one is a fully-nonstationary known counterpart modeled by a recorded earthquake, that takes into account the time variability of both intensity and frequency content; the second one is a corrective term represented by a stationary zero-mean Gaussian process adjusting the response spectrum of the nonstationary signal in order to make it spectrum compatible. That is,

$$\ddot{u}_g(t) = \alpha\, \ddot{u}_g^R(t) + \ddot{u}_g^S(t)\,, \tag{13}$$

where $\ddot{u}_g^R(t)$ is the recorded (R) earthquake time history that is assumed known, α is a scaling coefficient and $\ddot{u}_g^S(t)$ is the stochastic (S) corrective term whose power spectral density has to be determined. Accordingly, let consider the equation governing the motion of a single-degree-of-freedom system

$$\ddot{u}(t) + 2\zeta\omega_0\dot{u}(t) + \omega_0^2 u(t) = -(\alpha\, \ddot{u}_g^R(t) + \ddot{u}_g^S(t))\,. \tag{14}$$

The response displacement time-history can be cast in the form

$$u(t) = \alpha\, u^R(t) + u^S(t)\,, \tag{15}$$

whose counterparts are solution of the two independent differential equations

$$\ddot{u}^R(t) + 2\zeta\omega_0\dot{u}^R(t) + \omega_0^2 u^R(t) = -\ddot{u}_g^R\,, \tag{16}$$

$$\ddot{u}^S(t) + 2\zeta\omega_0\dot{u}^S(t) + \omega_0^2 u^S(t) = -\ddot{u}_g^S. \tag{17}$$

Accordingly, the response spectrum $RSA(\omega_0, \zeta)$ of the ground motion $\ddot{u}_g(t)$ given in eq. (13) can be approximately determined by the equation

$$RSA(\omega_0, \zeta) = \sqrt{\alpha^2 RSA^R(\omega_0, \zeta)^2 + RSA^S(\omega_0, \zeta)^2}\,, \tag{18}$$

where $RSA^R(\omega_0, \zeta)$ is the response spectrum of the recorded ground motions, $\ddot{u}_g^R(t)$, and $RSA^S(\omega_0, \zeta)$ is the response spectrum pertinent to the stochastic zero-mean stationary Gaussian process $,\ddot{u}_g^S(t)$. The latter can be approximately determined through the first crossing problem given by the equation

$$\begin{aligned} &RSA^S(\omega_0, \zeta) \\ &\quad = \omega_0^2 \eta_{U^S}(T_s, p = 0.5, \lambda_{0,U^S}(\omega_0, \zeta), \lambda_{0,U^S}(\omega_0, \zeta), \lambda_{1,U^S}(\omega_0, \zeta), \lambda_{2,U^S}(\omega_0, \zeta))\sqrt{\lambda_{0,U^S}(\omega_0, \zeta)} \end{aligned} \tag{19}$$

formally analogous to eq. (1). Let assume now that $RSA(\omega_0, \zeta)$ represents the known target response spectrum (i.e. defined by the seismic code). Combining eqs. (18) and (19), it follows that

$$\begin{aligned} &RSA(\omega_0, \zeta)^2 - \alpha^2 RSA^R(\omega_0, \zeta)^2 \\ &\quad = \omega_0^4 \eta_{U^S}^2(T_s, p = 0.5, \lambda_{0,U^S}(\omega_0, \zeta)\,, \lambda_{1,U^S}(\omega_0, \zeta)\,, \lambda_{2,U^S}(\omega_0, \zeta)\,)\lambda_{0,U^S}(\omega_0, \zeta) \\ &\qquad \forall\, RSA(\omega_0, \zeta) > \alpha\, RSA^{(R)}(\omega_0, \zeta) \end{aligned} \tag{20}$$

It has to be emphasized that equation (18) hold only if

$$RSA(\omega_0,\zeta) > \alpha\, RSA^{(R)}(\omega_0,\zeta) \tag{21}$$

Accordingly, in the case in which the response spectrum of the recorded ground motion is greater than the target response spectrum the coefficient α have to be less than 1. In order to respect eaquation (21) and to minimize the difference between the target and the recorded response spectrum the following value of the coefficient α is herein proposed

$$\alpha = \min\left\{\frac{RSA(\omega_0,\zeta)}{RSA^{(R)}(\omega_0,\zeta)}\right\}. \tag{22}$$

Note that, in the case in which response spectrum of the recorded ground motion is lower than the target response spectrum the coefficient α can be set equal to 1 for let the natural accelerograms unmodified. However, in the case in which the response spectrum of the natural accelerograms lies very below the target response spectrum equation (22) can be again retained for reducing the influence of the corrective term on the overall model.

Therefore, modifying the solution proposed in [17] the power spectral density of the corrective stochastic stationary process $\ddot{u}_g^S(t)$ is given by

$$G_{\ddot{u}_g}^S(\omega) = 0 \qquad 0 \le \omega \le \omega_l \ , \tag{23}$$

$$G_{\ddot{u}_g}^{S}(\omega_i)=\frac{4\zeta}{\omega_i\pi-4\zeta\omega_{i-1}}\mathcal{U}\left(\frac{RSA(\omega_i,\zeta)^2-\alpha^2\,RSA^R(\omega_i,\zeta)^2}{\eta_{U^S}^2(\omega_i,\zeta)}-\Delta\omega\sum_{j=1}^{i-1}G_{\ddot{u}_g}^{S}(\omega_j)\right)$$
$$\times\left(\frac{RSA(\omega_i,\zeta)^2-\alpha^2\,RSA^R(\omega_i,\zeta)^2}{\eta_{U^S}^2(\omega_i,\zeta)}-\Delta\omega\sum_{j=1}^{i-1}G_{\ddot{u}_g}^{S}(\omega_j)\right),\qquad \omega>\omega_l \tag{24}$$

with η_{U^S} approximately posed equal to η_U defined in eq. (2) and $\mathcal{U}(\bullet)$ is the unit step function, introduced for avoiding eventual negative solutions. After determining the spectrum compatible power spectral density $G_{\ddot{u}_g}^{S}(\omega)$ the simulation of fully nonstationary spectrum compatible ground acceleration earthquakes is performed via the equation

$$\ddot{u}_g^{(k)}(t)=\alpha\,\ddot{u}_g^{R}(t)+\varphi(t)\sum_{i=1}^{N_a}\sqrt{2G_{\ddot{u}_g}^{S}(i\,\Delta\omega)\Delta\omega}\cos(i\,\Delta\omega\,t+\phi_i^{(k)}) \tag{25}$$

where $\varphi(t)$ is the modulating function defined in equation (12). Depending on the recorded earthquake time history iterative improvement of the power spectral density of the corrective term could be necessary for satisfying code provisions. To this aim, by modifying eq. (10), the following iterative scheme is proposed

$$G_{\ddot{u}_g}^{S\,(j)}(\omega)=G_{\ddot{u}_g}^{S\,(j-1)}(\omega)\left[\frac{RSA(\omega,\zeta)^2}{\widetilde{RSA}^{(j-1)}(\omega,\zeta)^2}\right], \tag{26}$$

in which $\widetilde{RSA}^{(j)}(\omega,\zeta)$ represents the mean response spectrum of the ground acceleration $\ddot{u}_g(t)$ determined at the *j*-th iteration.

Remarkably, via the proposed procedure spectrum compatible fully nonstationary earthquakes in agreement with code provisions can be simulated. The nonstationary behavior relies on the recorded signal that would be chosen so as to reflect local geotech-

nical and seismological characteristics. The spectrum compatible criteria are satisfied by the superposition of the corrective quasi-stationary Gaussian random process whose power spectral density have been determined through a handy recursive formula.

4 INFLUENCE OF THE CORRECTIVE TERM

In previous sections it has been proposed an approach for generating fully nonstationary spectrum compatible earthquakes. By the proposed approach recorded time-histories are modified via a corrective term enhancing the frequency content of the original signal. In order to clarify how the corrective term modify the nonstationary content of the signal two parameters are scrutinized, namely the mean instantaneous energy and frequency [29]. The term instantaneous implies that both energy and frequency are valuated locally so as to describe their evolution in time. Specifically, it can be shown [30] that the mean instantaneous energy $\langle E(t) \rangle$ can be determined directly by the knowledge of the evolutionary power spectral density function $G_{\ddot{u}_g}(\omega,t)$ of the ground motion process by the equation

$$\langle E(t) \rangle = \lambda_{0,\ddot{u}_g}(t) = \int_0^\infty G_{\ddot{u}_g}(\omega,t) d\omega \tag{27}$$

where the brackets stands for mean value. Taking into account eq (13) and owing to the statistical independence of the random corrective term and the deterministic recorded earthquake, the following equation holds

$$G_{\ddot{u}_g}(\omega,t) = \hat{G}^R_{\ddot{u}_g}(\omega,t) + G^S_{\ddot{u}_g}(\omega,t)\,. \tag{28}$$

where $\hat{G}^R_{\ddot{u}_g}(\omega,t) = \alpha^2 G^R_{\ddot{u}_g}(\omega,t)$ is the scaled joint time-frequency distribution of the recorded accelerogram [29, 31-33], while $G^S_{\ddot{u}_g}(\omega,t)$ is the separable power spectral density of the corrective term given by the equation

$$G^S_{\ddot{u}_g}(\omega,t) = \varphi^2(t) G^S_{\ddot{u}_g}(\omega). \tag{29}$$

In which $\varphi(t)$ is the modulating function defined in eq (12) and $G^S_{\ddot{u}_g}(\omega)$ has been defined in equations (23) and (24). Furthermore, using equation (27) after simple algebra it can be shown that

$$\langle E(t)\rangle = \langle E^R(t)\rangle + \langle E^S(t)\rangle \tag{30}$$

where $\langle E^R(t)\rangle$ is the mean instantaneous energy of the recorded signal given by the equation

$$\langle E^R(t)\rangle = \int_0^\infty \hat{G}^R_{\ddot{u}_g}(\omega,t)\, d\omega \tag{31}$$

while $\langle E^S(t)\rangle$ is the mean instantaneous energy of the corrective term given by the equation

$$\langle E^S(t)\rangle = \lambda^S_{0,\ddot{u}_g}(t) = \varphi^2(t) \int_0^\infty G^S_{\ddot{u}_g}(\omega)\, d\omega \ , \tag{32}$$

Equation (30) emphasizes that the corrective term provides an increment of the original energy of the recorded signal, strictly related to the amplitude of the signal, measurable by the knowledge of equation (32).

In order to scrutinize the variation of the frequency content with respect to time the mean instantaneous frequency is introduced [29, 33, 34],

$$\left\langle \omega(t) \right\rangle = \frac{\int_0^\infty \omega G_{\ddot{u}_g}(\omega,t)d\omega}{\int_0^\infty G_{\ddot{u}_g}(\omega,t)d\omega} \tag{33}$$

By using the same arguments to determine the mean instantaneous energy, after simple algebra it can be shown that

$$\left\langle \omega(t) \right\rangle = \frac{\left\langle \omega^R(t) \right\rangle \left\langle E^R(t) \right\rangle + \left\langle \omega^S \right\rangle \left\langle E^S(t) \right\rangle}{\left\langle E^R(t) \right\rangle + \left\langle E^S(t) \right\rangle} \tag{34}$$

where $\left\langle \omega^R(t) \right\rangle$ is the mean instantaneous frequency of the original record given by the equation

$$\left\langle \omega^R(t) \right\rangle = \frac{\int_0^\infty \omega G^R_{\ddot{u}_g}(\omega,t)d\omega}{\int_0^\infty G^R_{\ddot{u}_g}(\omega,t)d\omega} \equiv \frac{\int_0^\infty \omega \hat{G}^R_{\ddot{u}_g}(\omega,t)d\omega}{\int_0^\infty \hat{G}^R_{\ddot{u}_g}(\omega,t)d\omega} \tag{35}$$

while $\left\langle \omega^S \right\rangle$ is the mean instantaneous frequency of the quasi-stationary corrective term, clearly independent with respect to time. The latter can be easily determined by the equation

$$\left\langle \omega^S \right\rangle = \frac{\int_0^\infty \omega G^S_{\ddot{u}_g}(\omega)d\omega}{\int_0^\infty G^S_{\ddot{u}_g}(\omega)d\omega} = \frac{\lambda^S_{1,\ddot{u}_g}}{\lambda^S_{0,\ddot{u}_g}} \equiv \omega_c^S \tag{36}$$

ω_c^S being the central frequency of the quasi-stationary corrective process. Equation (34) shows that the nonstationary frequency content of the original record manifested through the evolution of the mean instantaneous frequency $\left\langle \omega^R(t) \right\rangle$, is modified due the adding of the corrective term in a weighted mean sense. As a consequence the more the

mean instantaneous energy content of the corrective term is negligible the more the local nonstationary behavior of the simulated spectrum compatible earthquakes tends to that one pertaining to the original record.

5 NUMERICAL RESULTS

In this section the proposed method for generating fully nonstationary spectrum compatible earthquakes is applied to the target response spectrum defined in Eurocode 8 [2]. Specifically, for a 5% damping ratio the response spectrum is given by the equations

$$\begin{aligned} RSA(T) &= a_g S\left[1+\frac{T}{T_B}(1.5)\right] && 0 \le T \le T_B \\ RSA(T) &= 2.5 a_g\, S && T_B \le T \le T_C \\ RSA(T) &= 2.5\, a_g S\left[\frac{T_C}{T}\right] && T_C \le T \le T_D \\ RSA(T) &= 2.5\, a_g S\left[\frac{T_C T_D}{T^2}\right] && T_D \le T \le 4s \end{aligned} \tag{37}$$

According to Eurocode 8, consistency (i.e. spectrum compatibility) is considered to be achieved if the condition

$$\max\left\{\frac{\widetilde{RSA}(T)-RSA(T)}{RSA(T)}\times 100\right\} \le 10\% \tag{38}$$

is satisfied over the range of periods between $0.2T_1$ to $2T_1$; T_1 being the fundamental period of the structure under study in the direction where the accelerogram is applied; and if

$$\widetilde{RSA}(0) > a_g S\,, \tag{39}$$

$\widetilde{RSA}(T)$ being the mean response spectrum from at least three simulated earthquakes.

5.1 Example 1

In this numerical example Type B soil (deposits of very dense sand, gravel, or very stiff clayground) and Type 1 seismicity has been selected. Table 1 shows the pertinent response spectrum parameters. Furthermore, the maximum ground acceleration a_g it has been set equal to $0.35g$. Nonstationary characteristics have been modeled using the time-histories pertinent to two real earthquake records having quite different spectral content changing in time. The first record corresponds to the SOOE (N-S) component of the Imperial Valley earthquake of May 18, 1940, recorded at El Centro site. The second record is the NOOW (N-S) component of the san Fernando earthquake of February 9, 1971, recorded at Orion Boulevard site, extensively studied in reference [31].

5.1.1 *EL CENTRO 1940, NORTH-SOUTH COMPONENT*

El Centro (1940) earthquake is used first. Pertinent ground motion time history is plotted in Figure 1a. In order to apply the proposed procedure the duration of the time observing window T_s has to be set along with the parameters of the modulating function defined in equation (12). These parameters can be determined through the so called Husid function [36] defined by the equation

$$\mathcal{H}(t)=\frac{\int_0^t\left[\ddot{u}_g^R(t)\right]^2 dt}{\int_0^{t_f}\left[\ddot{u}_g^R(t)\right]^2 dt};\qquad 0\le\mathcal{H}(t)\le 1, \tag{40}$$

$t_f = 30\,s$ being the duration of the recorded earthquake ground motion. Accordingly, the duration of the strong motion phase, that will be assumed coincident to duration of the time-observing window, is $T_s = t_2 - t_1$, where t_1 and t_2 are the time instants in which $\mathcal{H}(t)$ is equal to 0.05 and 0.95, respectively. Figure 1b shows the evolution of the Husid function. Pertinent parameters are: $t_1 = 1.65\,s$, $t_2 = 25.51\,s$ and $T_s = 23.86\,\mathrm{s}$. Furthermore the parameter β defining the decay of the modulating function after t_2 has been set equal to $3/(t_f - t_2)$ so reducing the amplitude of the simulated signal of about 95% for $t = t_f$. Since the response spectrum of the recorded earthquake lies below the target one no scaling coefficient have been used for this example (i.e. $\alpha = 1$).

The stationary power spectral density function of the corrective stochastic process has been then determined via the proposed procedure and depicted in Figure 2. Just five iterations has been required for satisfying equation (38). One hundred spectrum compatible artificial earthquakes have been simulated by using equation (25) setting $N_a = 400$ and $\Delta\omega = 0.25\ rad/s$. Three trajectories are plotted in Figure 3 manifesting the randomness of the simulated accelerograms.

It is noted that the simulation of artificial accelerograms could lead to velocity and displacement trajectories possessing unrealistic drift. This phenomenon, widely addressed in literature for real earthquakes [36], have been also manifested in previous studies on the simulated accelerograms (see e.g.[14],[27]). It has to be emphasized that the correc-

tion of this physically unrealistic drift is crucial for the analysis of nonlinear behaving structures as well as linear behaving structures with very long period [14, 27]. To date there is no unique criterion for correcting the artificial accelerograms. A comparative study of many common techniques applied for correcting real earthquakes have been presented in [36]. Herein, a modified version of the second order polynomial baseline correction presented in [14] has been applied in this paper. Specifically, each individual simulated trajectory $\ddot{u}_g^{(k)}(t)$ is modified as follows

$$\ddot{\hat{u}}_g^{(k)}(t) = \ddot{u}_g^{(k)}(t) - (a_0 + a_1 t + a_2 t^2) \tag{41}$$

where the coefficients a_0, a_1, and a_2 of the polynomial have been herein determined approximating $\ddot{u}_g^{(k)}(t)$ in a least square sense. It is noted that this approach can be regarded as an application of a low band filter to the simulated trajectory $\ddot{u}_g^{(k)}(t)$. Figure 4 shows the physical reliable behavior of both velocity and displacement trajectories computed from a selected corrected accelerograms.

In order to check the suitability of the simulated artificial earthquakes according to EC8 provisions in Figure 5 the mean response spectrum is compared with the target response spectrum. The perfect matching manifests the accuracy of the proposed procedure and the suitability of the generated artificial accelerograms for design purposes.

For sake of clarity Figure 6 shows the flow chart of the procedure proposed for simulating the spectrum compatible accelerograms.

The nonstationary features of the artificial spectrum compatible earthquakes have been then scrutinized through the study of the joint time frequency power spectral density function. According to equation (28) the joint time-frequency power spectral density function is given by the superposition of two contributions. The first one is given by the

joint-time frequency distribution of the nonstationary natural accelerogram while the second one is given by the separable power spectrum of the random corrective term. The former contribution can be determined through various approaches (Short Time Fourier Transform, Wavelets Transform, etc.). A comprehensive study on the current procedures can be found in [29, 32, 33]. The analytical model proposed for the El Centro 1940 earthquake proposed by Conte and Peng [31] is used in this paper and depicted in Figure 7a. Figure 7b shows the separable power spectral density function of the corrective term determined through equations (12), (23), (24) and (29) while, in Figure 7c the spectrum compatible evolutionary power spectral density function of the artificial ground motion acceleration determined by the proposed approach through equation (28) is depicted. Furthermore, the mean instantaneous energy (Figure 8) and frequency (Figure 9) have been evaluated by using equations (30) and (34). Remarkably, the time variability of both these quantities manifests the fully nonstationary behavior of the spectrum compatible artificial accelerograms preserving also similar shape (distribution of peaks and valleys) of that determined for the original earthquake record.

5.1.2 *ORION BOULEVARD 1971, NORTH-SOUTH COMPONENT*

The proposed procedure for simulating fully nonstationary spectrum compatible earthquakes has been also applied to the Orion Boulevard 1971 earthquake record. Ground motion acceleration time history along with Husid function is depicted in Figures 10. Pertinent estimated parameters are: $t_1 = 3.94\,s$, $t_2 = 18.88\,s$ and $T_s = 14.94\,\mathrm{s}$. The stationary power spectral density function of the corrective stochastic process has been

then determined and depicted in Figure 11. Also in this case one hundred samples of the spectrum compatible artificial earthquakes have been simulated. Three of these trajectories are plotted in Figure 12. Evidence of the effectiveness of the baseline correction adopted can be found in Figure 13. The mean response spectrum has been then compared with the target response spectrum in order to check the suitability of the simulated artificial earthquakes according to EC8 provisions. Remarkably, the perfect matching showed in Figure 14 manifests the efficiency of the proposed procedure and the suitability of this second set of artificial accelerograms for design purposes.

Time variability of the spectral content of both original and modified spectrum compatible earthquakes is shown in Figures 15. Due the strong nonstationary characteristics of the Orion Boulevard 1971 ground acceleration record the influence of the corrective term is herein more evident. Nevertheless, the spectrum compatible artificial earthquakes still preserve fully nonstationary characteristics as shown in Figures 16 and 17.

5.2 Example 2

The two numerical examples shown in previous section posses the common characteristic that the response spectrum of the recorded accelerograms lies below the target response spectrum. Since the response spectra of both the accelerograms are very close to the target one at some frequencies, no scaling parameter has been used (i.e. $\alpha = 1$). In this numerical example the case in which the response spectral coordinates of the original recorded accelerogram attain higher values from the target spectrum at some frequencies/natural periods (for which the scaling parameter $\alpha < 1$ is required) and the case where the response spectral coordinates of the original recorded accelerogram lies

very below the target spectrum is addressed. Type A (Rock or other rock-like geological formation, including at most 5 m of weaker material at the surface.), and Type D (Deposits of loose-to-medium cohesionless soil, or of predominantly soft-to-firm cohesive soil) have been selected for this purpose. El Centro 1940 ground acceleration record has been also selected. For both cases the parameter α has been determined through equation (22) obtaining $\alpha = 0.44$ and $\alpha = 1.16$ for Type A and Type D response spectrum cases, respectively. Clearly, the value $\alpha = 0.44$, manifests that the response spectrum of El Centro 1940 earthquake attains values higher about twice the value the target response spectrum for a given natural frequency. After scaling the recorded accelerograms the procedure is applied. Figure 18 shows the accuracy of the proposed approach also in these cases. The joint time-frequency distribution of the El Centro 1940 earthquake is shown in Figures 19 and 20 pertaining Type A and Type D response spectra, respectively. By the comparison of Figures 19(a) and 19(b) it is observed that the corrective term represents the major contribution to the whole spectrum compatible power spectral density function. By the exam of Figures 20(a) and 20(b), on the other hand, the contribution of the corrective term appears comparable with the scaling joint time frequency distribution of the El Centro 1940 earthquake. This is clearly related to the different target response spectra considered. Furthermore, by the exam of Figures (19) and (20) it can be appreciated as the corrective term modifies the original time variability of both mean instantaneous energy and frequency. Specifically, the greater is the energy content of the quasi stationary corrective term, such as in the case response spectrum A, the greater is the difference between the original and the modified mean instantaneous energy and frequency functions.

6 CONCLUSIONS

In this paper a method for generating fully nonstationary spectrum compatible earthquakes has been proposed. The method is based on the spectral representation of stochastic processes. Specifically, it is assumed that the ground motion is modeled by the superposition of two contribution: the first one is a fully-nonstationary counterpart modeled by a recorded earthquake that takes into account the time variability of both intensity and frequency content; the second one is a corrective term represented by a stationary process adjusting the response spectrum of the nonstationary signal in order to make it spectrum compatible. The corrective term is determined using a handy recursive formula determining the pertinent power spectral density function. The method is quite versatile and it has provided accurate results in all the cases analyzed.

Remarkably, the simulated earthquakes do not require any further iterative correction leading the proposed procedure very handy and competitive from a computational point of view. Moreover the method allows to determine the evolutionary spectrum compatible power spectral density that can be used for reliability studies.

The influence of the corrective term on the nonstationary characteristics of the original record has been studied by the mean of both instantaneous energy and frequency time evolution. Interestingly, two sets of artificial earthquakes possessing quite different nonstationary characteristics and fulfilling Eurocode 8 provisions have been determined. Accordingly, both sets can be used for design purpose. Future works will be aimed to study the influence of this multiple solutions on the seismic assessment of structures.

REFERENCES

[1] International Conference of Building Officials, Uniform Building Code, Vol. 2, 1997.

[2] European Committee for Standardization, Eurocode 8: Design of structures for earthquake resistance -Part 1: General rules, seismic actions and rules for buildings¸ Brussels, Belgium 2003.

[3] Ahmadi G. Generation of artificial time-histories compatible with given response spectra – a review. SM archives 1979; 4(3): 207-239;

[4] Barenberg ME. Inelastic Response of a Spectrum-Compatible Artificial Accelerogram. Earthquake Spectra 1989; 5(3): 477-493

[5] Ghaboussi J, Lin C-CJ. New method of generating spectrum compatible accelerograms using neural networks. International Journal for Earthquake Engineering and Structural Dynamics 1998; 27:377 –396.

[6] Mukherjee S, Gupta VK. Wavelet-based generation of spectrum compatible time-histories, Soil Dynamics and Earthquake Engineering 2002; 22: 799-804.

[7] Suárez LE, Montejo LA. Generation of artificial earthquakes via the wavelet transform International Journal of Solids and Structures 2005; 42: 5905-5919 .

[8] Hancock J, Watson-Lamprey J, Abrahamson NA, Bommer JJ, Markatis A., Mccoy E, Mendis R. An improved method of matching response spectra of recorded earthquake ground motion using wavelets, Journal of Earthquake Engineering 2006; 10: 67-89.

[9] Vanmarcke EH, Gasparini DA. Simulated earthquake ground motions. Proc. 4th Int. Conf. on Smirt, K1/9, San Francisco1977.

[10] Kaul MJ. Stochastic Characterization of earthquakes through their response spectrum. Earthquake Engineering and Structural Dynamic 1978; 6: 497-509.

[11] Sundararajan C. An iterative method for generation of seismic power spectral density functions. Nuclear Engineering and Design 1980; 61: 13-23.

[12] Pfaffinger DD. Calculation of power spectra from response spectra, Journal of Engineering Mechanics 1983. 109(1): 357-372.

[13] Preumont A. A method for the generation of artificial earthquake accelerograms. Nuclear Engineering and Design 1980; 59: 357-368.

[14] Preumont A, The generation of spectrum compatible accelerograms for the design of nuclear power plants, Earthquake Engineering and structural Dynamic, 1984; 12, 481-497

[15] Der Kiureghian A, Neuenhofer A. A response spectrum method for multiple-support seismic excitation. Report No. UCB/EERC-91/08. Earthquake Engineering Research Center. University of California, Berkeley, CA, 1991.

[16] Di Paola M, La Mendola L. Dynamics of Structures under seismic input motion (eurocode 8). European Earthquake Engineering 1992; 2: 36-44

[17] Falsone G, Neri F. Stochastic modelling of earthquake excitation following the EC8: power spectrum and filtering equations. European Earthquake Engineering 2000, 1: 3-12.

[18] Cacciola P, Colajanni P, Muscolino G. Combination of modal responses consistent with seimic input representation. Journal of Structural Engineering 2004; 130(1): 47-55.

[19] Deodatis G. Non-stationary stochastic vector processes: seismic ground motion applications. Probabilistic Engineering Mechanics 1996; 11: 149-168.

[20] Shinozuka M. Stochastic Fields and their digital simulation, Stochastic Methods in Structural Dynamics (eds G.I. Schueller and M- Shinozuka), Martinus Nijhoff Publishers, Dordrecht 1987, 93-133.

[21] Yeh CH, Wen YK. Modeling of non-stationary ground motion and analysis of inelastic structural response. Structural Safety 1990; 8(1-4): 281-298.

[22] Wang J, Fan L, Qian S. and Zhou J. Simulations of non-stationary frequency content and its importance to seismic assessment of structures, Earthquake Engineering and Structural Dynamics 2002; 31: 993-1005.

[23] Spanos PD, Vargas Loli LM. A statistical approach to generation of design spectrum compatible earthquake time histories. Soil Dynamics and Earthquake Engineering 1985; 4(1), 2-8.

[24] Preumont A, The generation of nonseparable artificial earthquake accelerograms for the design of nuclear power plants, Nuclear Engineering and Design, 1985; 88, 59-67

[25] Shrinkhande M, Gupta VH. On Generating Ensemble of Design Spectrum-Compatible Accelerograms. European Earthquake Engineering 1996; 3: 49-56.

[26] Lin C-C J, Ghaboussi J. Generating multiple spectrum compatible accelerograms using stochastic neural networks. Earthquake Engineering Structural Dynamics 2001; 30: 1021-1042.

[27] Giaralis A and Spanos PD. Wavelets based response spectrum compatible synthesis of accelerograms- Eurocode application (EC8). Soil Dynamics and Earthquake Engineering, 2009, 29, 219-235.

[28] Jennings PC, Housner GW, Tsai C. Simulated earthquake motions for design purpose. Proc. 4th World Conference Earth. Eng. Santiago, vol. A-1: 145-160 1969.

[29] Cohen L. Time-Frequency Distributions – A Review. Proceedings of the IEEE 1989; 77(7): 941-981.

[30] Michaelov G, Sarkani S, Lutes LD. Spectral characteristics of nonstationary random processes – a critical review. Structural Safety 1999; 21: 223-244

[31] Conte JP, Peng BF. Fully nonstationary analytical earthquake ground-motion model, Journal of Engineering Mechanics 1997; 123(1): 15-24.

[32] Spanos PD, Failla G, Evolutionary spectra estimation using wavelets, Journal of Engineering Mechanics (ASCE), 2004; 130(8), 952-960

[33] Spanos PD, Giaralis A and Politis NP. Time- frequency representation of earthquake accelerograms and inelastic structural response records using the adaptive chirplet decomposition and empirical mode decomposition. Soil Dynamics and Earthquake Engineering, 2007, 27, 675- 689

[34] Spanos PD, Giaralis A, Politis NP and Roessett JM. Numerical treatment of seismic accelerograms and of inelastic seismic structural responses using harmonic wavelets. Computer-Aided Civil and Infrastructure Engineering, 2007, 22,254- 264.

[35] Husid RL. Analisis de terremotos – Analisis general, Revista del IDEM 1969, Santiago del Chile, 8: 21-42.

[36] Boore DM and Bommer JJ, Processing of strong-motion accelerograms: needs, options and consequences. Soil Dynamics and Earthquake Engineering, 2005, 25, 93-115.

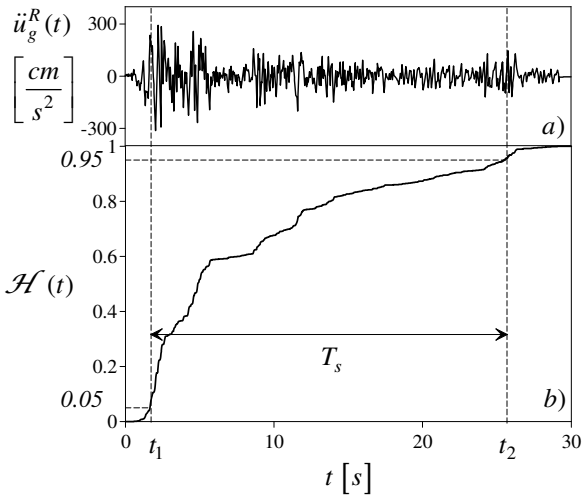

Fig.1 (a) Original ground acceleration time history and (b) Husid function of El Centro 1940 earthquake record

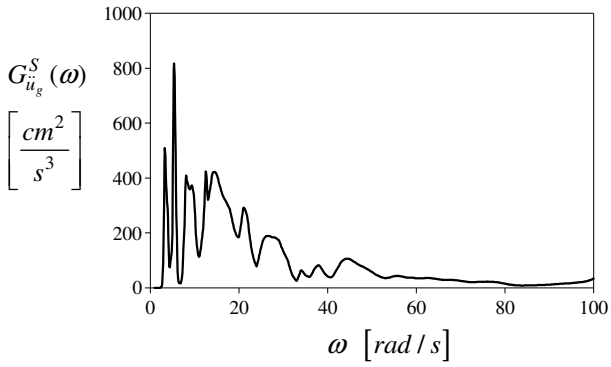

Fig.2 Stationary power spectral density function of the corrective stochastic process for El Centro 1940 earthquake ground acceleration

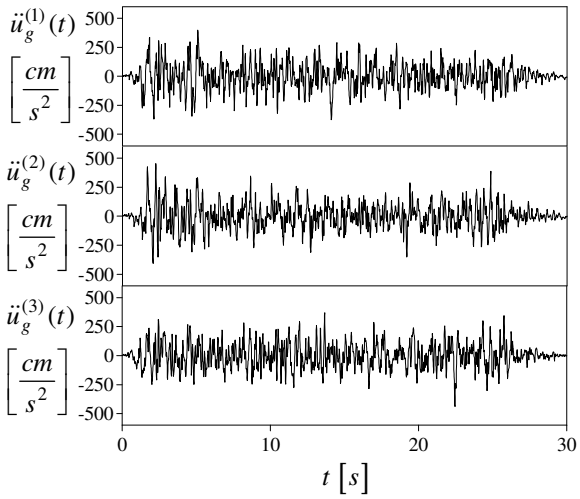

Fig.3 Artificial spectrum compatible ground acceleration time histories starting from El Centro 1940 earthquake record

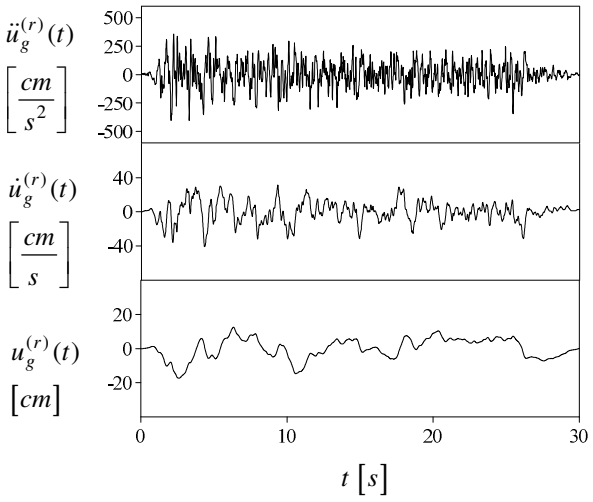

Fig.4 Samples of ground motion spectrum compatible acceleration, velocity and displacement time histories based on El Centro 1940 earthquake record compatible with Eurocode 8 type B response spectrum.

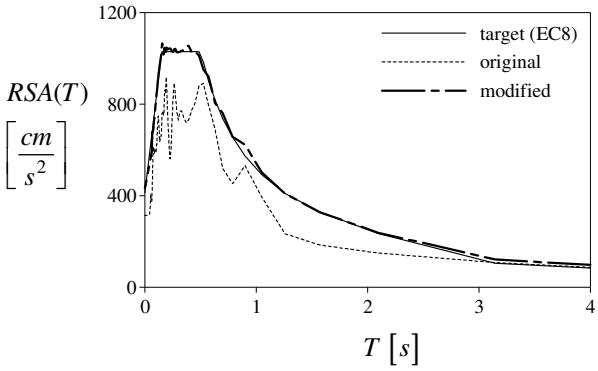

Fig.5 Comparison among the target response spectrum (EC8), the original response spectrum and the modified mean response spectrum of El Centro 1940 earthquake ground acceleration

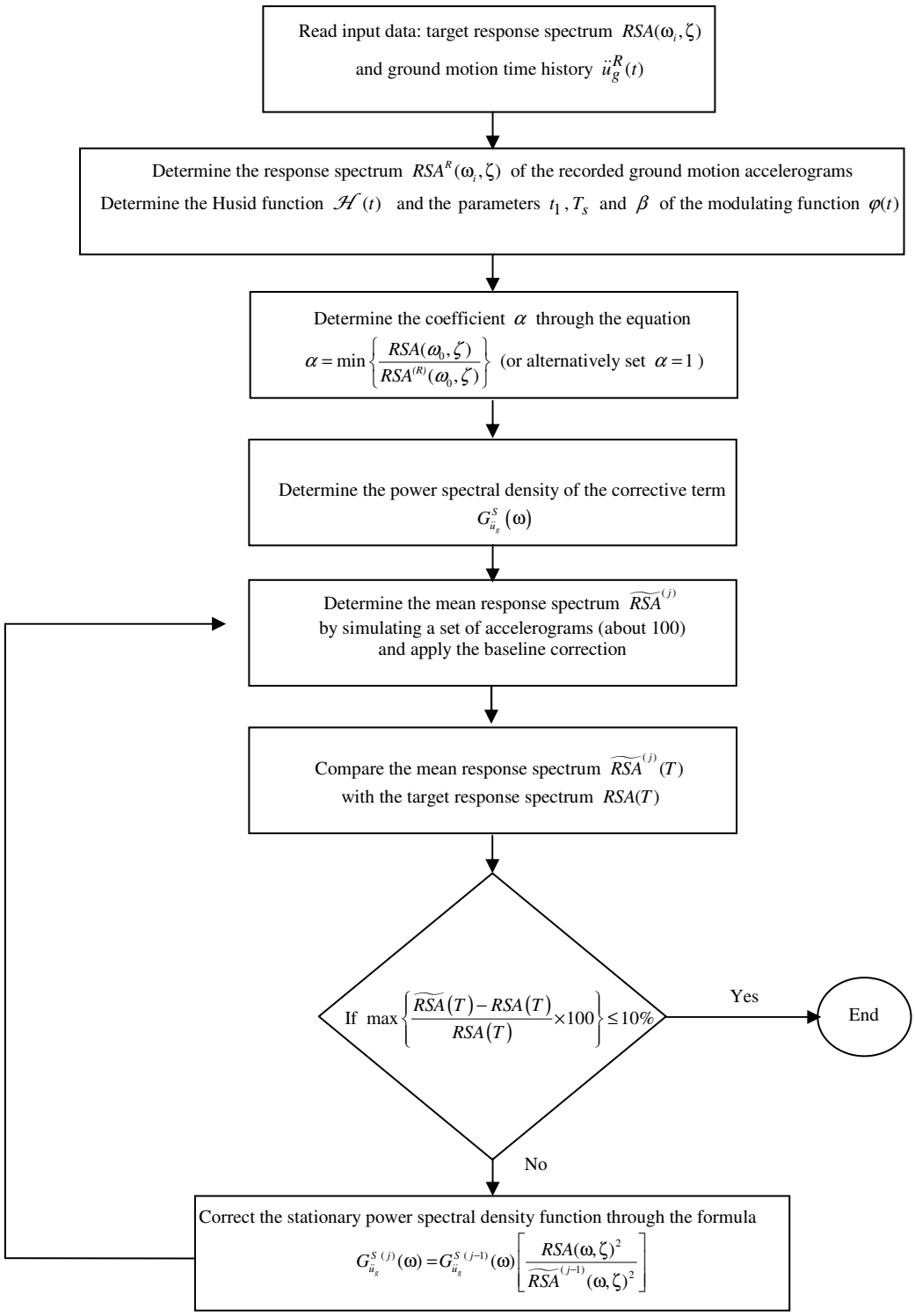

Fig.6 Flowchart of the proposed procedure for simulating fully non-stationary spectrum compatible accelerograms

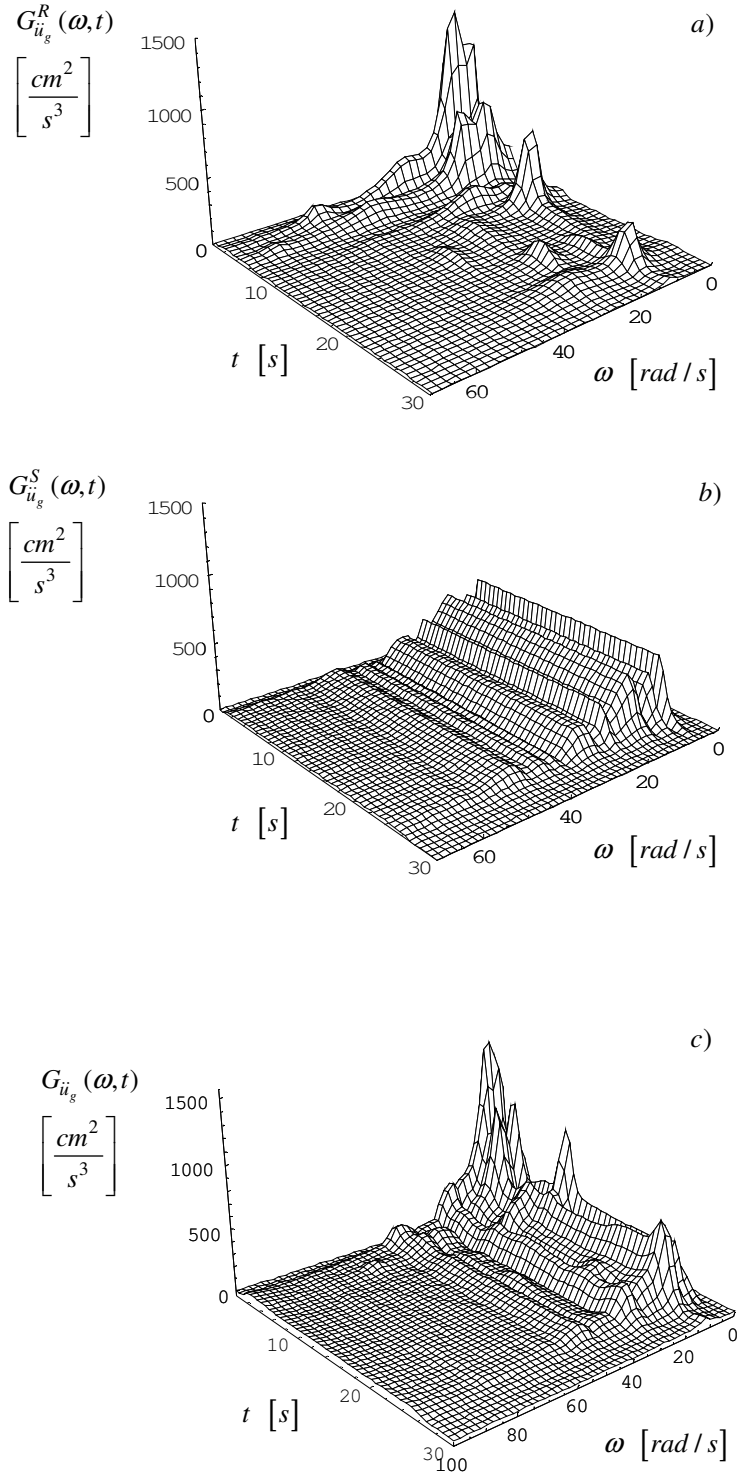

Fig.7 (a) Original time frequency distribution (after [31]) , (b) separable power spectral density of the corrective term and (c) evolutionary power spectral density based on El Centro 1940 earthquake ground with EC8 type B response spectrum.

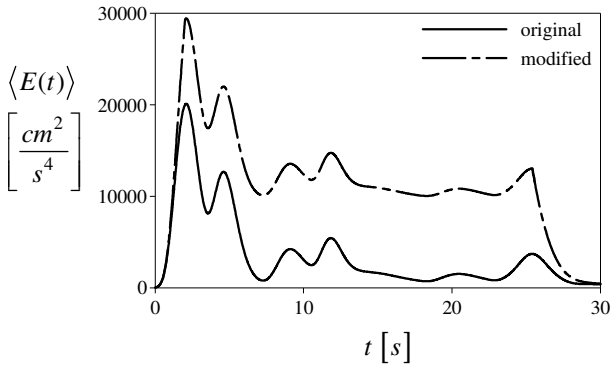

Fig.8 Comparison between original and modified mean instantaneous energy of El Centro 1940 earthquake ground acceleration

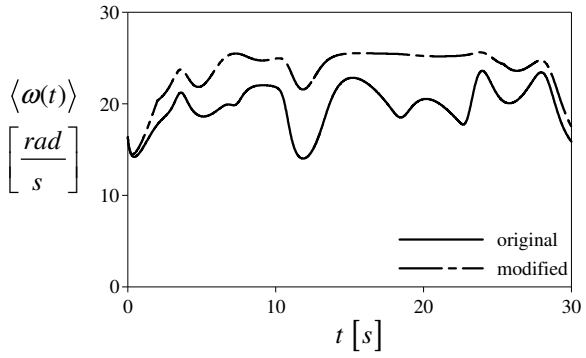

Fig.9 Comparison between original and modified mean instantaneous frequency of El Centro 1940 earthquake ground acceleration

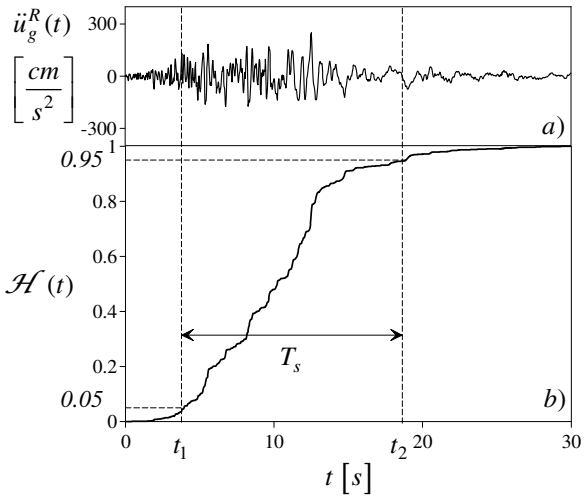

Fig.10 (a) Original ground acceleration time history and (b) Husid function of Orion Boulevard 1971 earthquake record

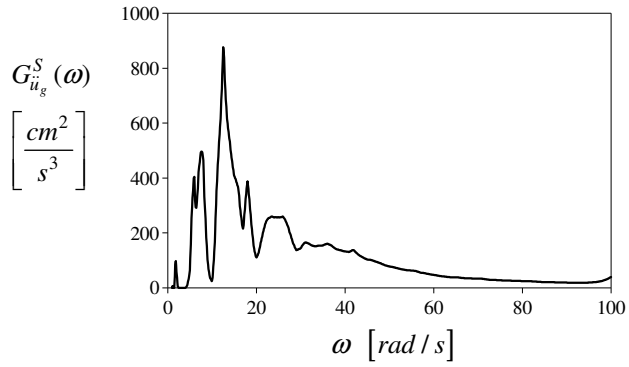

Fig.11 Stationary power spectral density function of the corrective stochastic process for Orion Boulevard 1971 earthquake ground acceleration

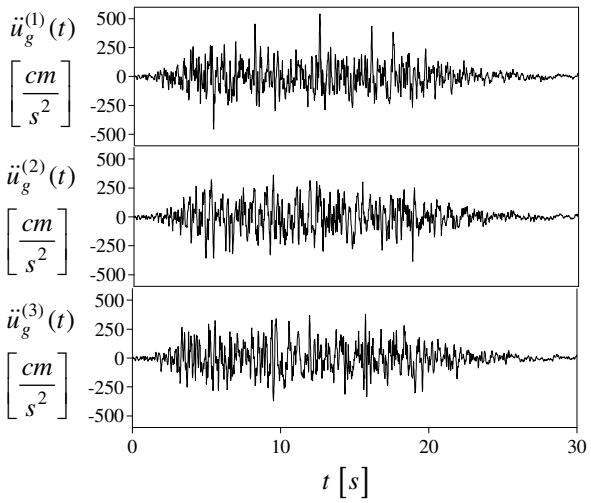

Fig.12 Artificial spectrum compatible ground acceleration time histories starting from Orion Boulevard 1971 earthquake record

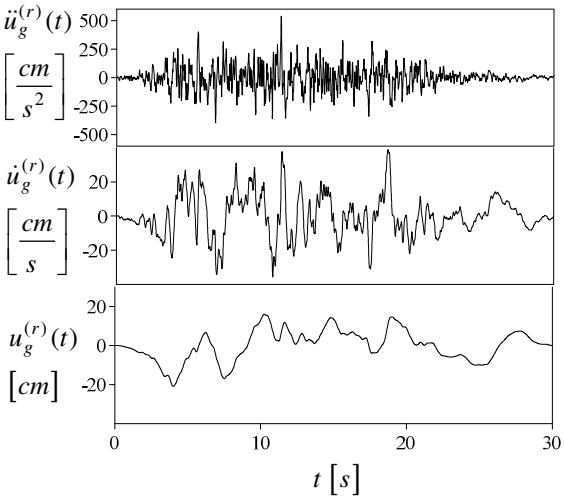

Fig.13 Samples of ground motion spectrum compatible acceleration, velocity and displacement time histories based on Orion Boulevard 1971 earthquake record compatible with Eurocode 8 type B response spectrum.

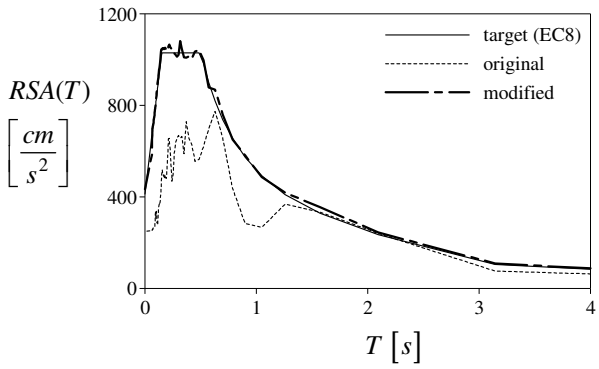

Fig.14 Comparison among the target response spectrum (EC8), the original response spectrum and the modified mean response spectrum of Orion Boulevard 1971 earthquake ground acceleration

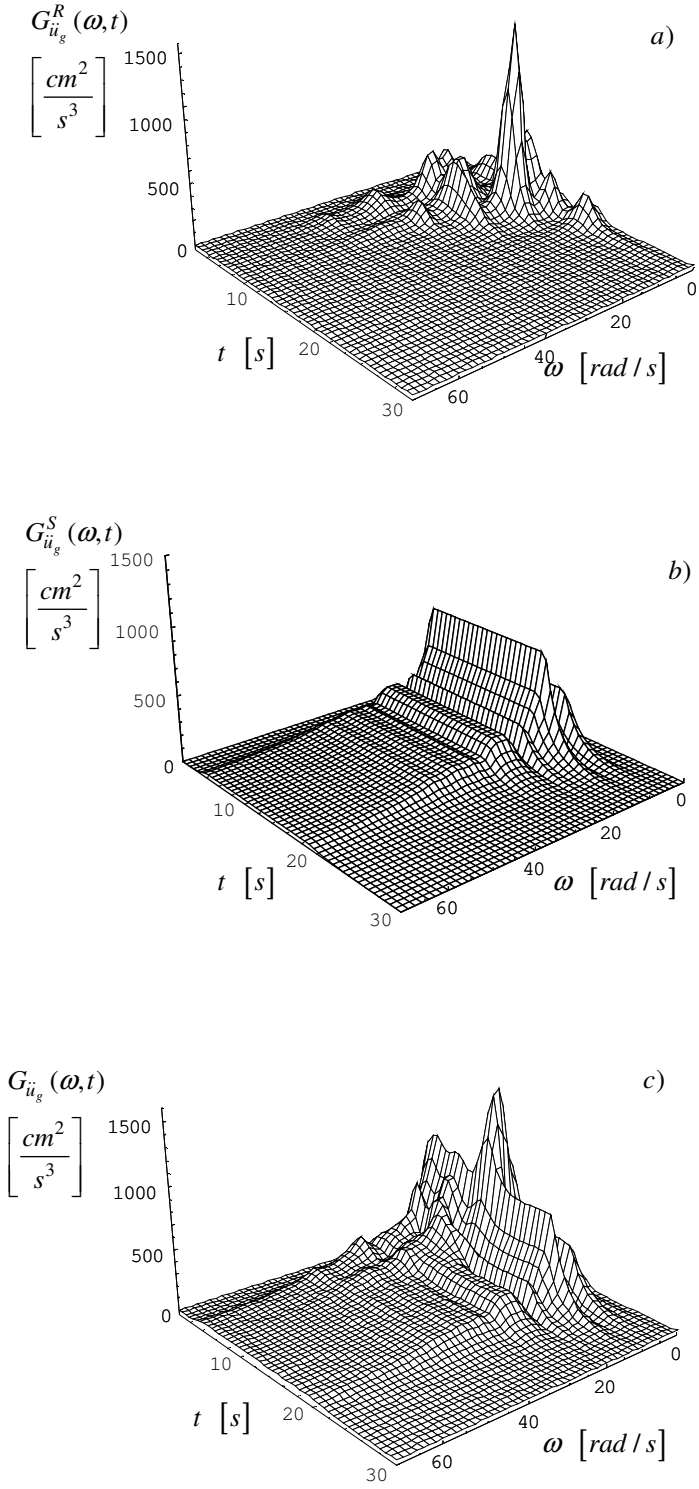

Fig.15 (a) Original time frequency distribution (after [31]) , (b) separable power spectral density of the corrective term and (c) evolutionary power spectral density based on Orion Boulevard 1971 earthquake compatible with EC8 type B response spectrum

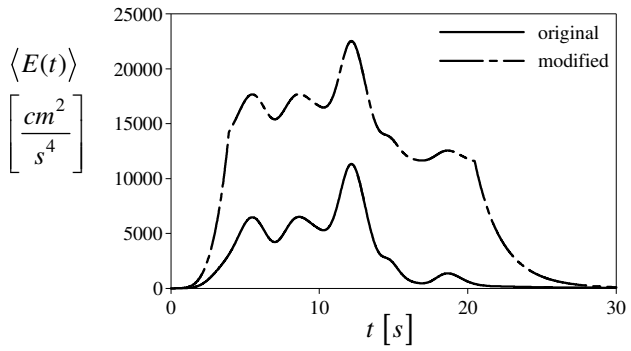

Fig.16 Comparison between original and modified mean instantaneous energy of Orion Boulevard 1971 earthquake ground acceleration

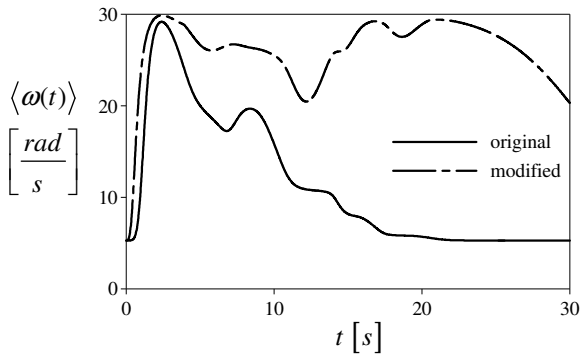

Fig.17 Comparison between original and modified mean instantaneous frequency of Orion Boulevard 1971 earthquake ground acceleration

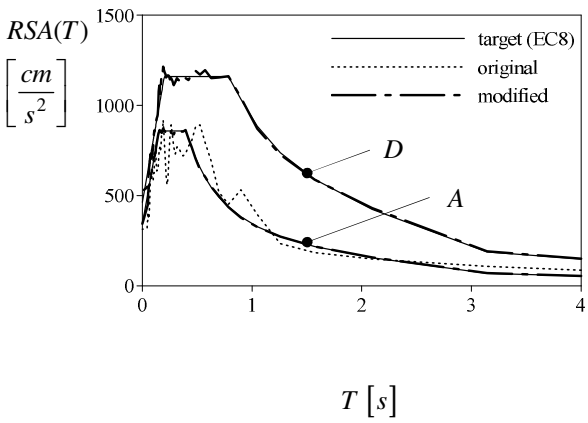

Fig.18 Comparison among target response spectra (EC8), the original response spectrum and the simulated mean response spectra based on El Centro 1940 earthquake ground acceleration

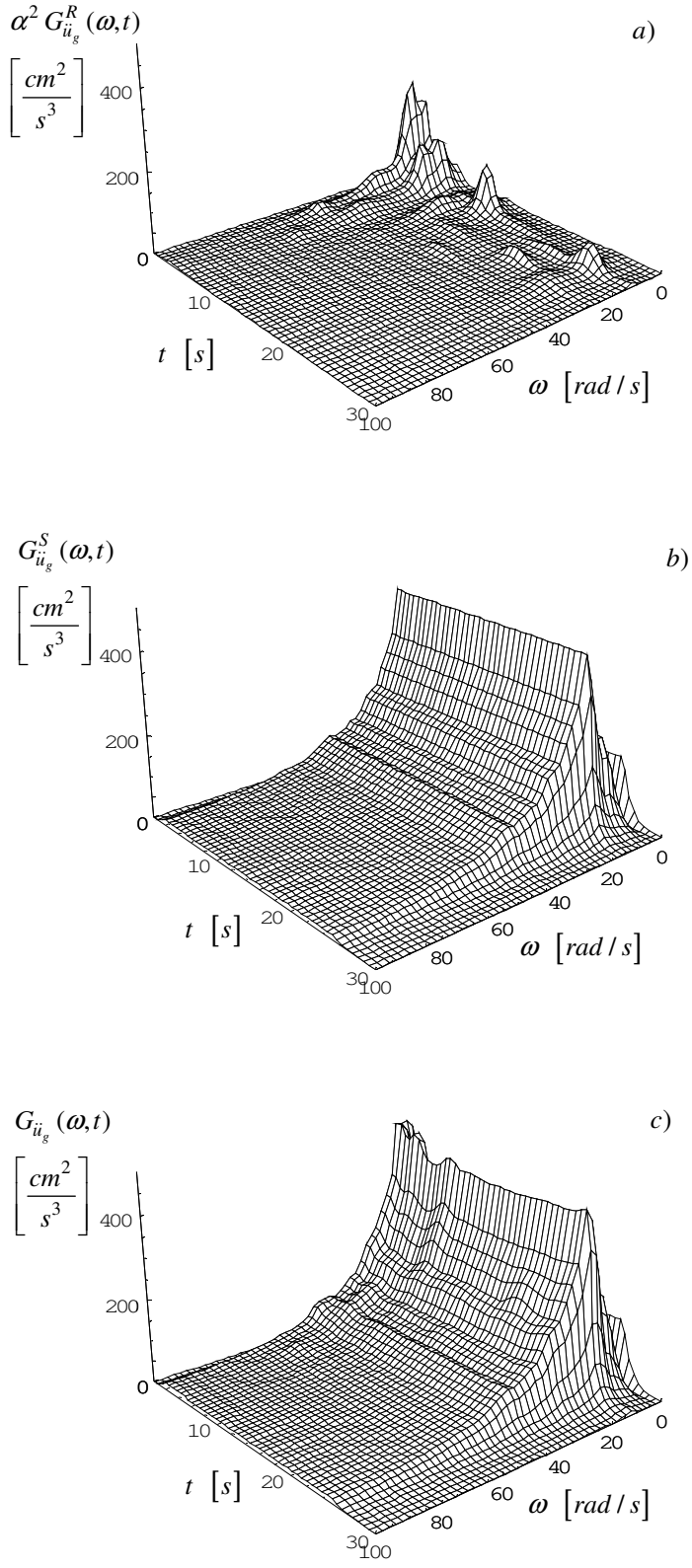

Fig.19 (a) Scaled ($\alpha = 0.44$) time frequency distribution (after [31]) , (b) separable power spectral density of the corrective term and (c) evolutionary power spectral density based on El Centro 1940 earthquake compatible with EC8 type A response spectrum.

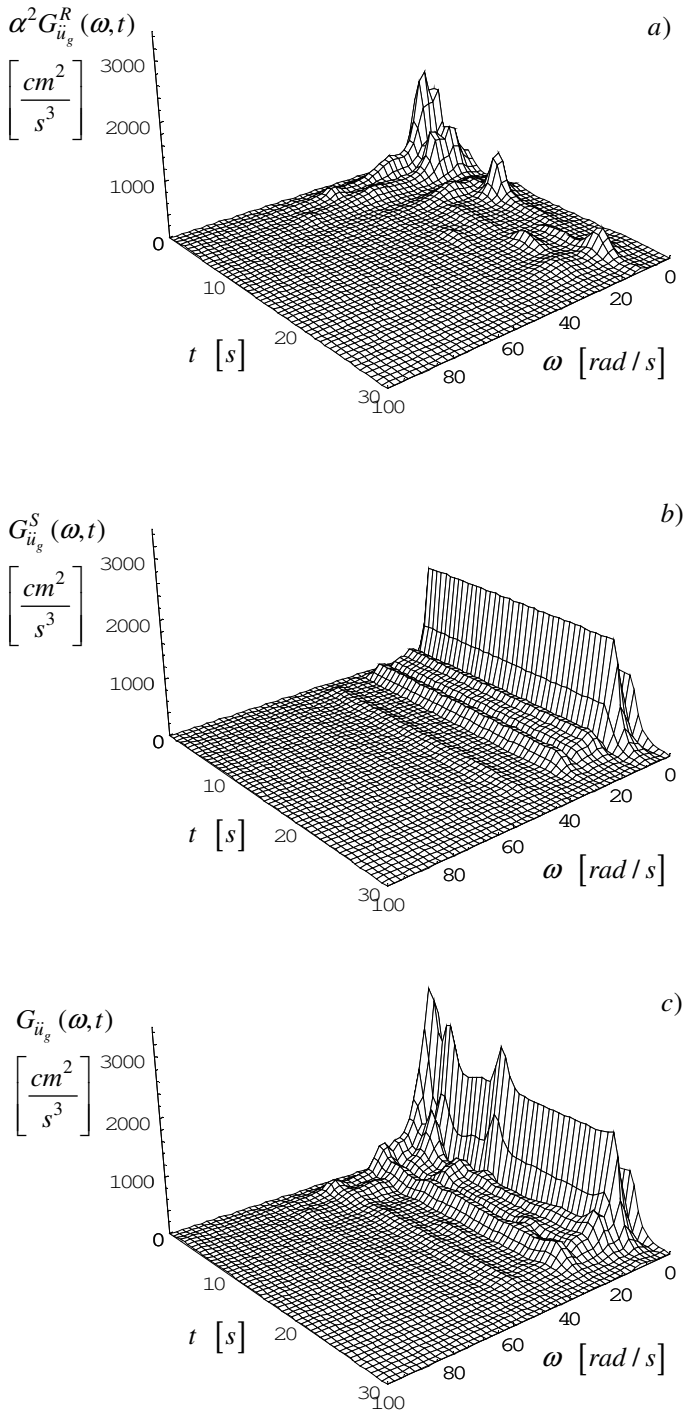

Fig.20 (a) Scaled ($\alpha = 1.16$) time frequency distribution (after [31]) , (b) separable power spectral density of the corrective term and (c) evolutionary power spectral density based on of El Centro 1940 earthquake compatible with EC8 type D response spectrum.

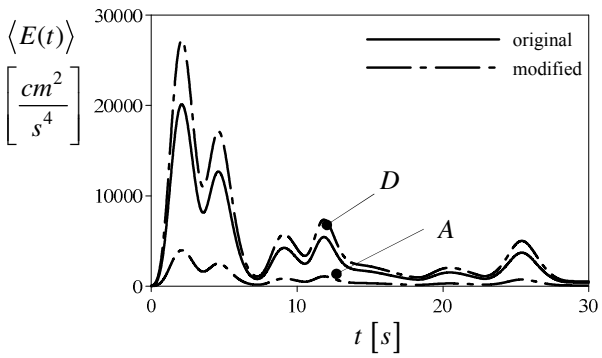

Fig.21Comparison between original and modified mean instantaneous energy of El Centro 1940 earthquake ground acceleration

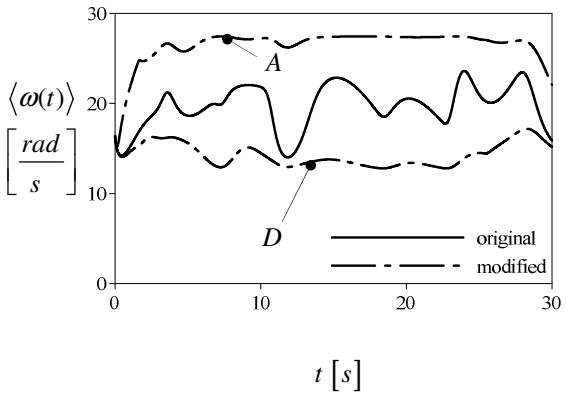

Fig.22 Comparison between original and modified mean instantaneous frequency of El Centro 1940 earthquake ground acceleration

Table 1: Values of the parameters describing the Eurocode 8 elastic response spectra for the selected ground type

Ground Type	S	$T_B[s]$	$T_C[s]$	$T_D[s]$
A	1.0	0.15	0.4	2.0
B	1.2	0.15	0.5	2.0
D	1.35	0.2	0.8	2.0